



Contents lists available at ScienceDirect

Catalysis Today

journal homepage: www.elsevier.com/locate/cattod

Oxidative dehydrogenation of ethane on diluted or promoted nickel oxide catalysts: Influence of the promoter/diluter

D. Delgado^a, B. Solsona^{b,*}, R. Sanchis^b, E. Rodríguez-Castellón^c, J.M. López Nieto^{a,*}

^a Instituto de Tecnología Química, Universitat Politècnica de València-Consejo Superior de Investigaciones Científicas, Avenida de los Naranjos s/n, 46022, Valencia, Spain

^b Departament d'Enginyeria Química, Universitat de València, C/ Dr. Moliner 50, 46100, Burjassot, Valencia, Spain

^c Departamento de Química Inorgánica, Facultad de Ciencias, Universidad de Málaga, 29071, Málaga, Spain

ARTICLE INFO

Keywords:

ODH of ethane
Supported nickel oxide
Promoted nickel oxide
Niobium oxide
Titanium oxide

ABSTRACT

Ti- and Nb- containing NiO catalysts have been synthesized by two different preparation methods: i) by precipitation (Me-Ni-O oxides, Me = Nb or Ti), in order to prepare promoted NiO catalysts; and ii) by wet impregnation on TiO₂ or NbO_x supports, in order to prepare diluted/supported NiO catalysts. The catalysts have been also characterized and tested in the oxidative dehydrogenation of ethane. The catalytic performance of Ti- and Nb-promoted catalysts strongly depends on the composition, although in both cases the optimal one is found at similar Ti or Nb loadings (ca. 90 wt% NiO), showing similar ethylene selectivity in the ODH of ethane (ca. 90% at 10–20% ethane conversion). However, in the case of diluted catalysts, the catalytic behavior of Ti- and Nb-containing catalysts is drastically different. Then, over TiO₂-diluted NiO catalyst, the highest selectivity to ethylene (ca. 90% selectivity) is achieved at NiO loading of 20 wt.%. However, over Nb₂O₅-diluted NiO catalyst, selectivity to ethylene was lower than 70%. A discussion on the characteristics of selective catalysts is done. In this case, the best catalysts must present a low concentration of free NiO and TiO₂ or Nb₂O₅ phases, maximizing the Ni-O-Ti or Ni-O-Nb interaction. Interestingly, this takes place at different NiO loading depending on the preparation method and the nature of promoter/diluter. The low selectivity to ethylene achieved by NiO diluted with Nb₂O₅ has been related to the low interaction of NiO with the surface of Nb₂O₅, which hinders the elimination of unselective electrophilic O species.

1. Introduction

The use of oil derivatives as fuels, especially in the automotive sector, is expected to decrease in Europe. In fact, this decrease is foreseen to be drastic from 2040, as several countries, such as Spain, UK, Denmark and Norway, have planned to ban vehicles fed with petrol and diesel. Therefore, the interest of oil and natural gas, especially as raw materials to be transformed into useful non-fuel products, is importantly increasing. Nowadays, ethylene, with a worldwide production of 150 million tons in 2015, can be considered as the most important feedstock in Petrochemistry [1]. Ethylene is mainly produced by steam cracking, a highly energy consuming and non-catalytic process [2,3]. The oxidative dehydrogenation (ODH) of ethane to ethylene using active and selective catalysts can be considered as an interesting alternative to the steam cracking process, due to the exothermic character of the reaction, the *in situ* reactivation of the catalysts and the relatively low reaction temperatures required [4,5]. Unfortunately, this process is not industrially developed, due to the fact that yields to ethylene are

still not high enough to displace the current non-catalytic process, but also for the risks associated to any technology shift, since steam-cracking is well-established and optimized process.

Modified NiO materials are, together with multicomponent MoV (Te,Sb)Nb oxides [6,7], the most promising catalysts for the ODH of ethane. Patents of Symix [8] and the pioneer works of Lemonidou et al. [9,10] with Ni-Nb-O catalysts firstly showed the high potential of this type of materials. In fact, ethylene yields over 45% have been reported.

Pure NiO easily activates ethane at low reaction temperatures (< 400 °C). Unfortunately, most of ethane is transformed into CO₂ and only a small fraction is converted into ethylene. Interestingly, the addition of several promoters to NiO has demonstrated to have a positive effect in the ethylene formation. We can mention metal oxide promoters as in the case of WO₃-NiO [11,12], CeO₂-NiO [13], ZrO₂-NiO [14], and Ta₂O₅-NiO [15] catalysts. The use of Sn [16,17] and, especially, Nb [18–22] as promoters of NiO leads to the best catalytic performance, achieving high selectivity to ethylene at moderate and high ethane conversions. In these promoted catalysts, mainly prepared by

* Corresponding author.

E-mail addresses: benjamin.solsona@uv.es (B. Solsona), jmlopez@itq.upv.es (J.M. López Nieto).

<https://doi.org/10.1016/j.cattod.2019.06.063>

Received 6 February 2019; Received in revised form 28 May 2019; Accepted 15 June 2019

0920-5861/ © 2019 Published by Elsevier B.V.

mixing solutions of the corresponding nickel and promoter salts, the formation of solid solutions and/or the partial incorporation of the promoter into the NiO lattice is favored. High valence of the foreign cation is suitable for achieving good performance, whereas the addition of alkalis and alkaline earths does not improve, or even worsen, the catalytic behavior compared to pure nickel oxide.

Although most of scientific papers deal with promoted NiO catalysts, supported/diluted NiO catalysts have also demonstrated to lead to high ethylene formation. Particularly, supports such as Al₂O₃ [23], porous clays [24], TiO₂ [25] or complex catalysts such as NiO-Al₂O₃/Ni-foam [26] have reached similar performance than optimal promoted NiO catalysts. In contrast, the use of silica, which allows only a weak NiO-support interaction, hardly modifies the poor behavior of pure NiO [24].

The reason for the drastic improvement observed in supported/diluted or promoted NiO catalysts compared to undoped NiO is not fully understood. Nevertheless, it is known that an excess of high valence Ni³⁺ species, the presence of non-stoichiometric oxygen species favors the undesired ethane deep oxidation [18,27,28]. The concentration of defects, mainly Ni and O vacancies, has also demonstrated to play an important role on the catalytic performance [12,29]. Overall the interaction between nickel and the promoter or diluter must be maximized whereas the amount of unmodified NiO sites must be minimized.

Nb⁵⁺ is probably the best promoter for NiO reported up to date, whereas TiO₂ can be considered among the best NiO supports for the ODH of ethane. Thus, in the present article we have followed two synthetic approaches, by which NiO has been promoted with Ti⁴⁺ or Nb⁵⁺ (in promoted NiO catalysts) or diluted with the corresponding oxides (i.e. TiO₂ or Nb₂O₅, in diluted catalysts), with the aim of understanding the role and main effects of promoters and diluters in the chemical nature of NiO. The results are presented taking into consideration changes in the chemical nature of NiO and its role in the catalytic behavior in the ODH of ethane.

2. Experimental

2.1. Catalyst synthesis

Diluted NiO/TiO₂ or NiO/Nb₂O₅ catalysts were prepared through the evaporation at 60 °C of a stirred ethanolic solution of Ni(NO₃)₂·6H₂O (from Sigma-Aldrich) and oxalic acid (oxalic acid/Ni molar ratio of 3) to which the corresponding titanium or niobium oxide was added. The solids obtained were dried overnight at 120 °C and finally calcined in static air at 500 °C for 2 h. The catalysts have been named as xNiO/Y, in which x is the theoretical NiO wt% loading and Y the diluter employed (TiO₂ or Nb₂O₅).

The TiO₂ support employed (Degussa P25) mainly consists of anatase (low proportion of rutile) and presents a surface area of 55 m² g⁻¹. Nb₂O₅ support was prepared by hydrothermal synthesis. An aqueous solution of ammonium niobate(V) oxalate hydrate (Sigma Aldrich) was heat treated at 80 °C for 10 min, and subsequently introduced in a Teflon-lined stainless steel autoclave, which was heat-treated at 175 °C for 48 h. Finally, the resulting solid was filtered, washed with distilled water, dried (16 h at 100 °C) and heat-treated under N₂ flow for 2 h at 550 °C (66 m² g⁻¹).

Promoted Ni-Ti-O and Ni-Nb-O catalysts were prepared by evaporating an ethanolic mixture of nickel nitrate Ni(NO₃)₂·6H₂O (Sigma-Aldrich), niobium oxalate monooxalate adduct C₁₀H₅NbO₂₀ (ABCR) or titanium ethoxide C₈H₂₀O₄Ti (ACROS) and oxalic acid (oxalic acid/Ni molar ratio of 3). The pastes obtained were dried overnight in a furnace at 120 °C and then calcined in static air at 500 °C for 2 h. The catalysts have been named as xNi-Ti-O or xNi-Nb-O, in which x is the theoretical NiO wt% loading.

Detailed synthesis procedures for both promoted and supported NiO catalysts are included in Supporting Information.

2.2. Catalytic tests in the ODH of ethane

Ethane oxidation tests were conducted in a tubular isothermal flow reactor, mainly in the 350–450 °C temperature range. The feed consisted of a mixture of C₂H₆/O₂/He with a molar ratio of 3/1/26. The contact times were varied by modifying the catalyst weight or the total flow in order to obtain the desired conversions at a given reaction temperature. Catalysts were introduced in the reactor together with silicon carbide in order to reach a constant volume in the catalytic bed. Reactants and reaction products have been analyzed by gas chromatography. Two packed columns were necessary to carry out the analyses: (i) molecular sieve 5 Å (2.5 m); and (ii) Porapak Q (3 m). Blank runs in the absence of catalyst showed no conversion in the range of reaction temperatures studied. Further details of the reaction system are included in Supporting Information.

2.3. Characterization techniques

N₂-adsorption isotherms were collected in a Micromeritics ASAP 2000. Approximately 300 mg of sample were degassed in vacuum at 400 °C prior to nitrogen adsorption. Surface areas were calculated by BET method.

X-ray diffraction patterns were measured in Bragg-Brentano geometry in a PANalytical X'Pert PRO diffractometer with an X'Celerator detector. Diffractograms were collected using Cu-K_α radiation.

Raman spectra were obtained in an inVia Renishaw spectrometer equipped with a Renishaw HPNIR laser, at an excitation wavelength of 514 nm. Power on the samples was of ca. 15 mW.

XPS studies were carried out on a Physical Electronics PHI VersaProbe II spectrometer using monochromatic Al-K_α radiation (49.1 W, 15 kV and 1486.6 eV) for analyzing the core-level signals of the elements of interest with a hemispherical multichannel analyzer. The energy scale of the spectrometer was calibrated using Cu 2p_{3/2}, Ag 3d_{5/2} and Au 4f_{7/2} photoelectron lines at 932.7, 368.2 and 84.0 eV, respectively. Under a constant pass energy mode at 23.5 eV condition, the Au 4f_{7/2} line was recorded with 0.73 eV FWHM at a binding energy (BE) of 84.0 eV. The X-ray photoelectron spectra obtained were analyzed using PHI SmartSoft software and processed using MultiPak 9.3 package. The binding energy values were referenced to adventitious carbon C 1s signal (284.8 eV). Shirley-type background and Gauss-Lorentz curves were used to determine the binding energies.

X-ray absorption measurements in the Ni K-edge were carried out at CLAES line at ALBA synchrotron (Barcelona, Spain). Spectra were collected from 8200 to 9175 eV. The optimum mass amount of each catalyst (i.e. the one to maximize signal-to-noise ratio; Ln(I₀/I₁) ≈ 1) was diluted in boron nitride and pressed into wafers. Spectra normalization was carried out in Athena software.

Temperature-programmed reduction in H₂ was performed in a Micromeritics Autochem 2910 device, which was equipped with a TCD detector. A mixture 10% H₂ in Ar was used to perform the reduction (total flow of 50 mL min⁻¹). Samples were heated up to 800 °C at a heating rate of 10 °C min⁻¹.

Scanning Electron Microscopy (SEM) images were collected in a JEOL 6300 Microscope, equipped with an Oxford LINK ISIS system to perform compositional analysis by energy-dispersive X-ray Spectroscopy (EDX)

3. Results and discussion

3.1. Catalytic performance in the ODH of ethane

As Nb-promoted NiO samples are possibly the most efficient nickel oxide catalysts for the ODH of ethane to ethylene [9], we wanted to know if supporting/diluting NiO on Nb₂O₅ by a wet impregnation method could have similar effect on the catalytic properties than standard Nb-promoted NiO catalysts. Thus, a set of NiO catalysts

Table 1

Catalytic results in the ODH of ethane obtained by supported/diluted NiO/TiO₂ and NiO/Nb₂O₅ catalysts prepared by wet impregnation^a.

Catalyst	Surface area (m ² g ⁻¹)	NiO (wt. %)	Ethane conversion (%)	Selectivity to ethylene (%)	Ethylene productivity ^c
NiO	15.4	100	7.5	33.3	339
92NiO/TiO ₂	40.2	92	15.5	64.2	1360
80NiO/TiO ₂	51.4	80	16.3	75.5	1683
50NiO/TiO ₂	46.6	50	15.9 ^b	87.0	946
20NiO/TiO ₂	50.4	20	11.9 ^b	89.3	726
5NiO/TiO ₂	52.2	5	6.4 ^b	84.7	371
TiO ₂	55.4	0	1.9 ^b	55.4	72.0
98NiO/Nb ₂ O ₅	n.a.	98	20.5	58.6	1642
92NiO/Nb ₂ O ₅	39.9	82	21.1	58.8	1696
80NiO/Nb ₂ O ₅	n.a.	80	18.7	63.4	1621
50NiO/Nb ₂ O ₅	61.2	50	13.4	59.7	1094
20NiO/Nb ₂ O ₅	65.0	20	10.1	59.2	817
5NiO/Nb ₂ O ₅	n.a.	5	3.2	48.3	211
Nb ₂ O ₅	66.4	0	0.6 ^b	0	0

^a At 450 °C and a contact time, W/F, of 2 g_{cat} h mol_{C₂}⁻¹.

^b At 450 °C and a contact time, W/F, of 4 g_{cat} h mol_{C₂}⁻¹.

^c Formation rate of ethylene as g_{C₂H₄}/kg_{cat} h.

supported on Nb₂O₅ (NiO/Nb₂O₅ series) was synthesized with different NiO loadings and compared with Nb-promoted NiO catalysts (Ni-Nb-O series). On the other hand, NiO/TiO₂ catalysts have shown one of the most promising results in the ODH of ethane among all supported NiO systems [25]. Accordingly, series of promoted (Ni-Ti-O) and diluted (NiO/TiO₂) nickel oxide catalysts with different NiO loadings have been prepared and tested in the oxidative dehydrogenation of ethane.

The catalytic results in the ODH of ethane for diluted and promoted catalysts with different NiO contents are summarized in Tables 1 and 2, respectively. Fig. 1 shows the variation of the selectivity to ethylene (measured at an ethane conversion of ca. 10%) as a function of NiO-loading for Nb- and Ti-containing catalysts, prepared by evaporation (promoted series) or by impregnation (diluted series).

Considering Nb-containing materials, the catalytic behavior differs for Nb-promoted and Nb₂O₅-diluted catalysts (Fig. 1A). In the case of promoted series, the selectivity to ethylene gradually increases with NiO-loading, reaching a maximum of 90% at NiO-loadings of 92 wt%. On the other hand, Nb₂O₅-diluted materials present much lower ethylene selectivity (in the 48–64% range) regardless of the amount of NiO loaded. Nevertheless, the selectivity to ethylene in the ODH of ethane notably increases by both synthetic approaches, compared to unmodified NiO (S_{ethylene} = 33.3%).

A different trend is observed for Ti-promoted and TiO₂-diluted

Table 2

Catalytic results in the ODH of ethane obtained over Ti- and Nb-promoted NiO catalysts^a.

Catalyst	Surface area (m ² g ⁻¹)	NiO wt.%	Ethane conversion (%)	Selectivity to ethylene (%)	Ethylene productivity ^c
NiO	15.4	100	7.5	33.3	339
98Ni-Ti-O	n.d.	98	17.2 ^b	68.4	804
92Ni-Ti-O	122	92	14.0	88.1	1686
80Ni-Ti-O	n.d.	80	17.6	84.3	2028
50Ni-Ti-O	129	50	17.5 ^b	79.9	955
20Ni-Ti-O	58.9	20	6.2 ^b	83.7	354
97Ni-Nb-O	n.a.	97	21.4	74.3	2174
92Ni-Nb-O	157	92	18.5	86.2	2180
80Ni-Nb-O	n.a.	80	13.3	86.3	1569
50Ni-Nb-O	107	50	4.1	87.5	491
20Ni-Nb-O	31.6	20	0.9	90.8	112

^a At 450 °C and a contact time, W/F, of 2 g_{cat} h mol_{C₂}⁻¹.

^b At 450 °C and a contact time, W/F, of 4 g_{cat} h mol_{C₂}⁻¹.

^c Formation rate of ethylene as g_{C₂H₄}/kg_{cat} h.

catalysts (Fig. 1B). In both cases a high selectivity to ethylene can be reached, either by promoting with Ti (92Ni-Ti-O, ca. 90% selectivity to ethylene) (Table 1), or by diluting nickel oxide with TiO₂ (20NiO/TiO₂, ca. 90% selectivity to ethylene) (Table 2). The variation of the selectivity to ethylene with NiO-loading in Ti-promoted series follows a similar trend than that observed in Nb-promoted materials, i.e. the selectivity progressively increases with NiO in the catalysts, attaining its maximum value at NiO loading of 92 wt% (Table 1) (Fig. 1B). On the contrary TiO₂-diluted nickel oxide materials displayed a different trend, in which the selectivity to ethylene progressively increases, reaching a maximum at NiO-loadings of 20 wt% (Fig. 1B). In this way, 20NiO/TiO₂ sample shows a selectivity comparable to the one obtained with the best Ti-promoted catalysts (92Ni-Ti-O). Then, both the synthesis procedures (i.e. evaporation or impregnation) and NiO-loading have an important effect on the nature of active sites available in each series of catalysts.

One of the key aspects in the development of effective catalysts for the ODH of ethane is to study the evolution of the selectivity to the olefin when the conversion of ethane increases. This is a crucial point when the aim is achieving high yields to ethylene in ethane ODH, since ethylene tends to react on non-selective sites to give carbon oxides in most of the catalytic systems reported in literature.

Fig. 2 shows the evolution of the selectivity to ethylene with the ethane conversion (at 450 °C) for representative diluted and promoted NiO catalysts (Fig. 2A and B, respectively). Unmodified NiO shows a very low selectivity to ethylene (ca. 35%), being CO₂ the main reaction product. The non-detection of CO in the output stream has been reported to be due to the relatively low reactivity of ethylene over these catalysts (i.e. a low tendency of NiO-based materials to ethylene deep oxidation) [30]. The fact that ethylene selectivity does not substantially decrease when increasing ethane conversion (even on this non-selective unmodified NiO catalyst) would be in line with this assumption. However, nickel oxide has been also reported to be a highly efficient catalyst in the oxidation of CO to CO₂, which is able to perform at much lower reaction temperatures than those applied in the present study [31,32].

When nickel oxide is dispersed using TiO₂ and Nb₂O₅ as diluters, the selectivity to ethylene in the ODH of ethane increases drastically, up to 60–70% in the less selective catalysts, and up to 90% selectivity in the most selective ones (i.e. 20 NiO/TiO₂) (Fig. 2A). More importantly, the selectivity to ethylene remains almost constant in all cases when ethane conversion increases. We can tentatively ascribe this effect to the absence of those non-selective sites that deeply oxidize ethylene to CO₂. This behavior is also observed in Nb- and Ti-promoted catalysts with high NiO-loadings (92Ni-Nb-O and 92Ni-Ti-O samples), which are the most selective catalysts within promoted series. On the contrary, a decrease in the selectivity to ethylene when ethane conversion increases is observed on those promoted catalysts with low NiO-loadings. In this case, the decreasing trend indicates ethylene decomposition, due to the consecutive transformation of the olefin to carbon oxides.

The formation rate of ethylene (STY) has also been determined on these catalysts (Figure S1). The variation of STY with NiO-loading follows the same trend regardless of the synthetic procedure and the promoter/diluter used. Thus, the productivity increases drastically even at very low amounts of diluter/promoter, likely due to the observed increase of the selectivity to ethylene (even at NiO loadings near 100 wt %). According to the different physicochemical features observed along NiO-based catalyst series, the fact that the catalytic activity does not vary proportionally with NiO content in the materials can be explained in terms of the different surface areas and NiO particle size, which would lead to different amounts of exposed active sites, as it will be discussed below. Overall, it has been observed that the catalytic performance strongly depends on both the preparation method (diluted or promoted catalysts) and on the nickel content.

High selectivity to ethylene can be obtained using Ni-Ti catalysts prepared either by impregnation (diluted NiO/TiO₂ catalysts) or by evaporation of solutions (promoted Ni-Ti-O). However, while achieving

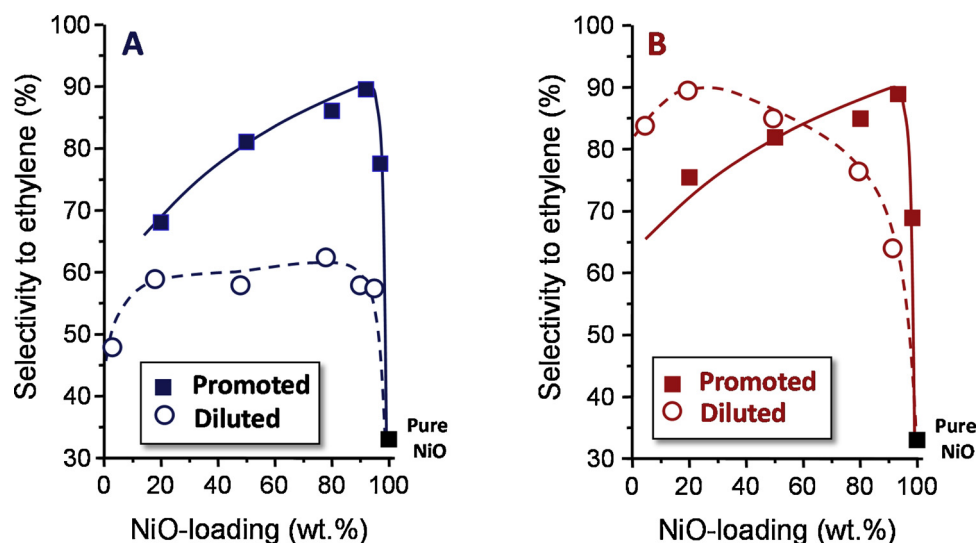


Fig. 1. Selectivity to ethylene in the ODH of ethane as a function of NiO-loading for promoted/diluted NiO catalysts: A) xNb-Ni-O and xNiO/Nb₂O₅-series; B) xTi-Ni-O and xNiO/TiO₂-series. Reaction conditions in text.

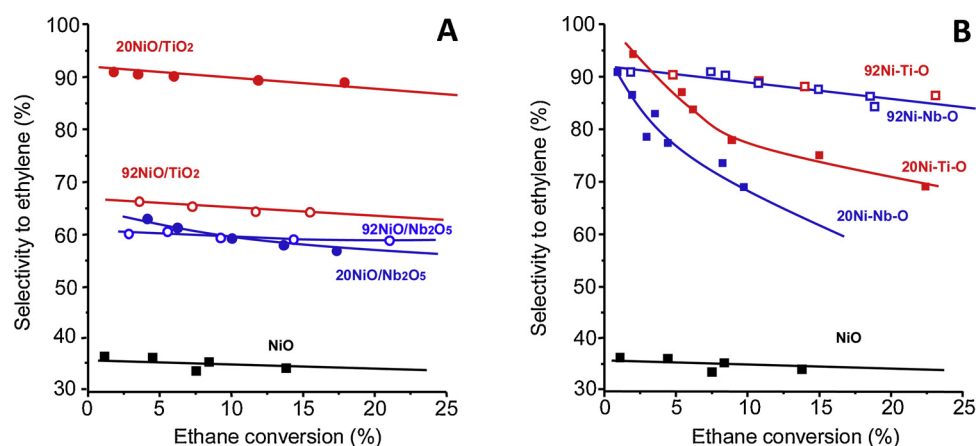


Fig. 2. Variation of the selectivity to ethylene with ethane conversion during the ODH of ethane for selected diluted (A) and promoted (B) NiO catalysts. Reaction conditions in text. Temperature = 450 °C.

similar selectivity to ethylene, different NiO-loadings are required depending on the synthetic approach chosen. Thus, much lower NiO loadings are needed in the case of diluted catalysts (20 wt% NiO) than in the case of Ti-promoted NiO (92 wt% NiO). It must be noted that NiO-loading must not be too high, in order to avoid ethane total oxidation, but neither too low, in order to prevent the ethylene decomposition into CO₂. As similar selectivity vs conversion profiles are observed in the optimal catalysts of each series, similar or equivalent Ni-Ti interactions must be taking place. The optimal Ni-loading is different in each case (for promoted and diluted catalysts), likely because an important part of TiO₂ support cannot interact with nickel oxide (i.e. the presence of non-accessible bulk Ti sites).

In the case of Ni-Nb materials, the catalytic behavior highly differs depending on the preparation method. Thus, when using promoted Ni-Nb-O catalysts with the appropriate composition, a high selectivity to ethylene can be attained. On the contrary, the selectivity to ethylene on NiO/Nb₂O₅ catalysts hardly exceeds 60%. Then it seems that the interaction between nickel oxide and niobium is different in diluted and promoted catalysts. The reason for the poor catalytic performance of diluted NiO/Nb₂O₅ mainly arises from the low initial selectivity to ethylene, due to the direct decomposition of ethane into carbon dioxide. In promoted Ni-Nb-O catalysts the selectivity achieved is high, but the amount of nickel must be controlled in order to avoid both ethylene decomposition (if nickel content is too low) and ethane total

oxidation (if nickel content is too high).

3.2. Physicochemical characterization of promoted and diluted NiO catalysts

Surface areas of both diluted and promoted catalysts were determined by BET method from N₂-adsorption isotherms (Table 1). Unmodified NiO presents low surface area (15 m²/g). In the case of diluted catalysts, two supports/diluters with similar surface area were used to deposit NiO (i.e. TiO₂ and Nb₂O₅, with surface area of 55 and 66 m²/g, respectively). When nickel is added by impregnation to both metal oxides, a progressive decrease in the surface area is observed as the nickel content increases (Table 1) (Fig. S2).

On the other hand, promoted catalysts (prepared by evaporation of solutions) show higher surface areas (over 100 m²/g) than diluted catalysts (Table 2) (Fig. S1). BET surface areas increase ten-fold even at low promoter contents (8 wt%, i.e. 92 wt% NiO loading), and decreases with the amount of Ni loaded (Table 2) (Fig. S2).

XRD patterns of diluted and promoted NiO-based catalysts are depicted in Figure S3 and Figure S4, respectively (see Supporting Information). In the case of NiO/TiO₂ (Fig. S3, A) and NiO/Nb₂O₅ (Fig. S3, B) series, all the materials show Bragg reflections corresponding to NiO cubic phase (Fm3m, ICSD No: 184626), together with the characteristics diffraction signals of the corresponding diluter oxide used in

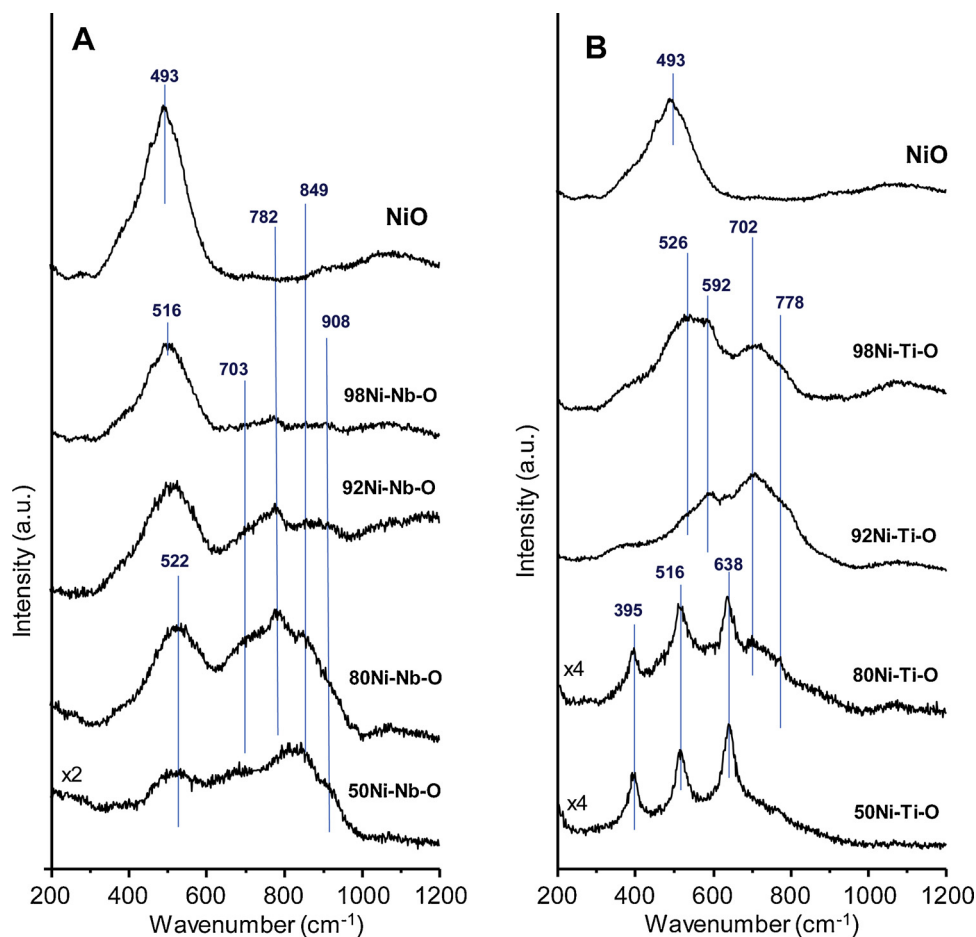


Fig. 3. Raman spectra of Nb- (A) and Ti- (B) promoted NiO catalysts.

each case, i.e. TiO_2 -P25 (showing a mixture of anatase and rutile-type phases) [33], and a highly distorted niobium oxide [34] (Fig. S3). On the other hand, promoted Ni-Nb-O and Ni-Ti-O catalysts present different structural features in comparison with diluted series, showing a comparable trend regardless of whether Nb or Ti are incorporated as promoters (Fig. S4, A and Fig. S4, B; respectively). At low promoter contents (NiO contents in the 0–80 wt% range), either for Ti-promoted or Nb-promoted series, the catalysts display the only presence of diffraction lines corresponding to NiO (Fig. S4, A; patterns a to d). At higher promoter concentrations (NiO wt% of 50 and 20%) additional features appear in the diffraction patterns. In the case of Nb-promoted catalysts, broad diffraction peaks are found at ca. $2\theta = 20\text{--}40^\circ$, which suggest the presence of amorphous niobium oxide [35] (Fig. S4, A; patterns d and f). For Ni-Ti-O series, TiO_2 -anatase diffraction signals (JCPDS: 84-1286) are found at these promoter contents (NiO wt% of 50 and 20%) (Fig. S4, B; patterns e and f). All these observations suggest a limit in the incorporation of both Ti and Nb within nickel oxide framework, after which simple titanium and niobium oxides are found as secondary phases. Nevertheless, according to broad features observed in the diffraction patterns, the presence of other Ni-promoter mixed oxide phases cannot be ruled out, as it will be discussed below.

Focusing on the possible effects of the promoter/diluter on the structural characteristics of NiO, we have calculated both average crystallite size (by using Scherrer equation) and a -parameter (by profile fitting). The results for both promoted and diluted catalysts are summarized in Table S1. A decrease in the crystallite size of NiO ($d_{\text{NiO}} = 25$ nm) is observed in all cases. This fact can be deduced from NiO line broadening found for all promoted and diluted materials. Interestingly, promoted catalysts show a smaller particle size ($d = 6.5\text{--}9.9$ nm), i.e. broader diffraction peaks, than diluted catalyst

($d = 12.4\text{--}15.1$ nm). Also, a slight increase in NiO a lattice parameter is observed in all modified NiO materials (Table S1). Again, the effect is more significant in Ni-Nb-O and Ni-Ti-O promoted series. Thus, the use of promoters seems to modify the original crystal framework and morphological characteristics of NiO in a higher extent than diluters do.

To get further insights into promoter/diluter-NiO interactions, selected samples were analyzed by Raman spectroscopy. Fig. 3 displays Raman spectra of promoted Ni-Ti-O and Ni-Nb-O catalysts (Fig. 3A and B, respectively). Unpromoted/undiluted NiO shows a main Raman band centered at 493 cm^{-1} , associated to Ni-O deformation modes [36] (Fig. 3, spectrum a). The original position of this band is shifted to higher frequencies (up to ca. 520 cm^{-1}) when Nb and Ti are added as promoters, even at low promoter concentrations (Fig. 3, spectra b and c). At higher promoter contents, Raman signals associated to the presence of Nb_2O_5 (band centered at 703 cm^{-1}) [37] and TiO_2 -anatase (bands at 395 , 516 and 638 cm^{-1}) [38] are also observed for Ni-Nb-O and Ni-Ti-O catalysts, respectively (Fig. 3, spectra d and e). Interestingly, additional features appear in the $600\text{--}900\text{ cm}^{-1}$ range in both Nb and Ti-promoted materials. In the case of Nb-promoted series, the spectra of the catalysts display bands at 782 and 849 cm^{-1} , ascribed to the presence of Ni-Nb-O mixed phases [39] and a signal at 908 cm^{-1} , attributed to Nb = O stretching vibrations [40] (Fig. 3A). In the same way, Ti-promoted catalysts present Raman bands centered at 702 and 778 cm^{-1} , which can be also assigned to mixed Ni-Ti-O oxide, specifically to an ilmenite NiTiO_3 -type phase [41] (Fig. 3B). Moreover, applying a higher heat-treatment temperature (i.e. 700°C), this ilmenite-type phase is clearly identified by X-ray diffraction (JCPDS: 33-0960) (Fig. S5).

In the case of diluted-NiO catalysts, both NiO/ TiO_2 and NiO/ Nb_2O_5 present common features in the Raman spectra, which are different

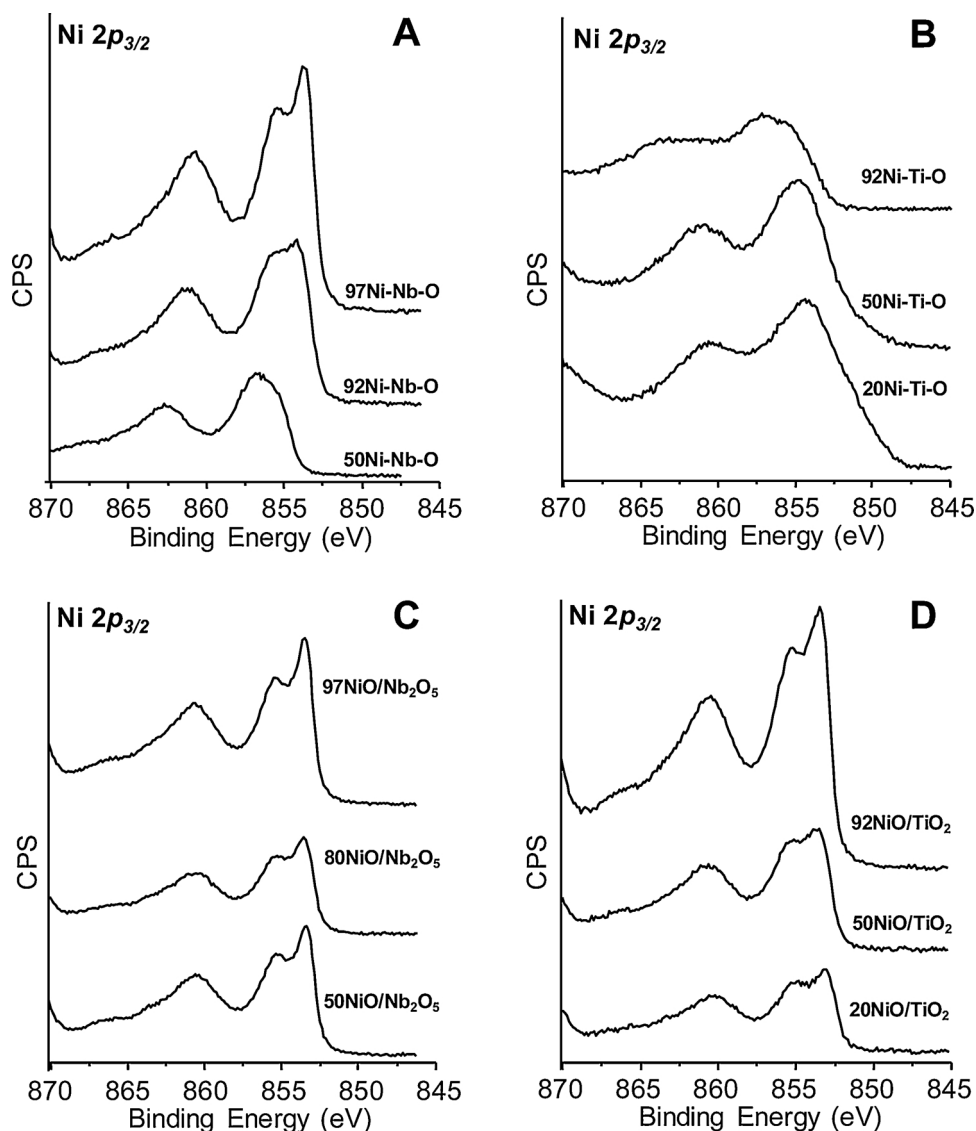


Fig. 4. Ni $2p_{3/2}$ core level spectra of promoted and diluted NiO catalysts. A) Ni-Nb-O series. B) Ni-Ti-O series. C) NiO/Nb₂O₅ series. D) NiO/TiO₂ series.

than those found in promoted NiO catalysts (see Fig. S6 in Supporting Information). In this sense, both series show always Raman band corresponding to NiO (ca. 493 cm^{-1}), which is not shifted regardless the diluter content used. In addition, they displayed characteristic Raman signals of each diluter added, i.e. a highly distorted Nb₂O₅ (700 cm^{-1}) (Fig. S6, A) and TiO₂-P25 (395, 515 and 638 cm^{-1}) (Fig. S6, B).

To evaluate possible modifications in the nature of nickel and oxygen surface species, selected catalysts were characterized by XPS. Fig. 4 shows the Ni $2p_{3/2}$ core level spectra of diluted and promoted catalysts. All the spectra show the typical NiO features, displaying a main peak in the 853–854 eV range, which shows line-broadening, which is generally considered a new peak (ca. 1.5 eV over the main signal), known as satellite I (Sat I). This Sat I has been reported to appear due to the presence of a wide variety of defects, such as Ni³⁺ species [42], Ni²⁺-OH sites or Ni²⁺ vacancies [43]. In addition to Sat I, another broad shake-up satellite (Sat 2) appears at ca. 7 eV over the main peak, which is generally attributed to ligand-metal charge transfer [43–45].

According to the complex nature of the NiO system, derived principally from its non-stoichiometric nature, it is difficult to discriminate among all the species that actually contribute to the XPS spectra in each case. Nevertheless, a decrease in the relative intensity of the main peak with respect to Sat I is observed along all the series of promoted and

diluted NiO catalysts (Fig. 4). This effect is more evident in Ni-Nb-O and Ni-Ti-O materials than in the case of diluted NiO/Nb₂O₅ and NiO/TiO₂, suggesting that promoters are able to modify the chemical nature of surface nickel species in a higher degree than diluters.

Fig. 5 displays the corresponding O 1s core level spectra of promoted and diluted NiO catalysts. The spectra of unpromoted/undiluted NiO presents two contributions, appearing at binding energy values of 529.4 and 531.1 eV, which can be assigned to nucleophilic and electrophilic surface oxygen species, respectively (Fig. S7) [46].

The effect of nucleophilic and electrophilic oxygen sites constitutes one of the central points in selective oxidation [47]. In this way, nucleophilic lattice oxygen (i.e. O²⁻) has been reported to be responsible for the partial oxidation of the substrate, meanwhile electrophilic oxygen species (likely O- or adsorbed O₂-) are prone to deep oxidation [48]. In this case, there exists a general trend among all analyzed diluted and promoted catalysts. Thereby, the XPS signal at B.E = 531.1 eV, corresponding to electrophilic oxygen species, decreases for the most selective catalysts (Fig. 5) (Table S2 and Figs. S8 and S9 in Supporting Information). Conversely, diluted NiO/Nb₂O₅ catalysts show the highest relative intensity of this signal, and the lowest selectivity to ethylene from all the series.

Surface Ni content for diluted and supported materials was calculated from XPS spectra (Table S2). For promoted catalysts and TiO₂-

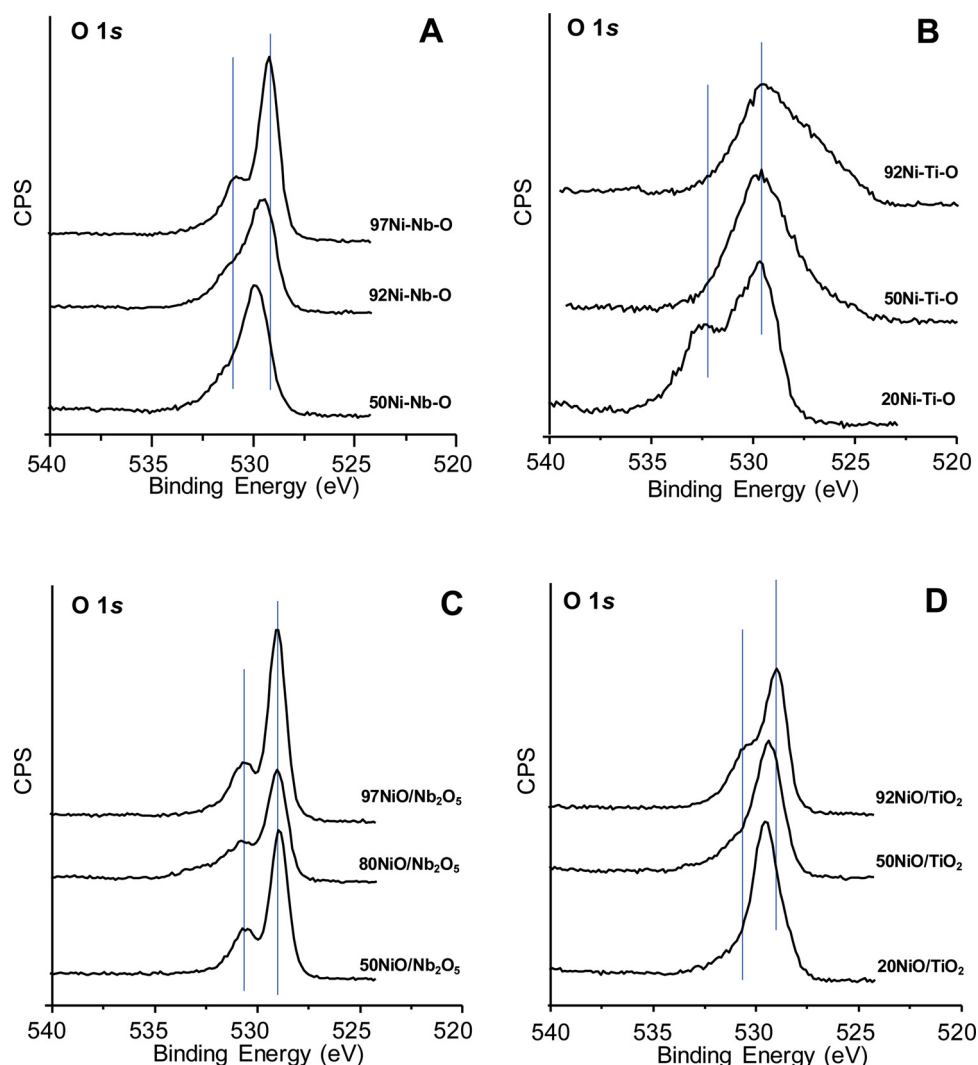


Fig. 5. O 1s core level spectra of promoted and diluted NiO catalysts. A) Ni-Nb-O series. B) Ni-Ti-O series. C) NiO/Nb₂O₅ series. D) NiO/TiO₂ series.

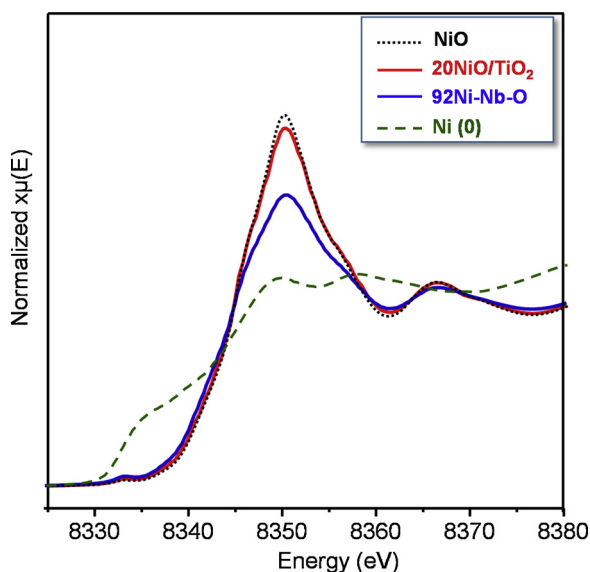


Fig. 6. XANES region of XAS spectra in the Ni K-edge of the most selective (sample 92Ni-Nb-O sample) and diluted (20NiO/TiO₂ sample) catalysts. For comparison, unmodified NiO and metallic nickel are also presented.

supported series, surface Ni concentrations increases proportionally with Ni-loading in the samples. However, Nb₂O₅-supported samples show high surface Ni contents, regardless of the amount of Ni loaded in the synthesis. We analyzed selected samples from NiO/TiO₂ and NiO/Nb₂O₅ series by SEM-EDX (Figs. S10 and S11). While TiO₂-supported NiO catalysts show a homogeneous Ni-content in all cases, Nb₂O₅-supported catalysts present a highly heterogeneous Ni-concentration all along the samples.

Hence, both diluters and promoters would act as modifiers of the O²⁻ sub-lattice, by eliminating the more electrophilic species, and improving the selectivity to ethylene in the ODH of ethane. The extent of this interaction will mainly depend on the nature of the support/diluter. Nb⁵⁺ and Ti⁴⁺ can be considered as high valence dopants within the pristine NiO framework, then pushing Ni to its lower oxidation state, i.e. Ni²⁺, thus decreasing the number of electrophilic oxygen species [28]. On the other hand, when using diluters instead of promoters, this will depend fundamentally on the ability of the diluter (TiO₂-P25 and Nb₂O₅) to interact with NiO.

With the aim of gaining additional information about the chemical nature of nickel species, selected catalysts were analyzed by X-ray absorption spectroscopy (XAS). Specifically, we have focused our attention into XANES features in XAS spectra, which are highly dependent on the electronic properties of the absorbing atom. Fig. 6 displays XANES region of the XAS spectra in the Ni K-edge of unmodified NiO (i.e. unselective in the ODH of ethane) and 20NiO/TiO₂ and 92Ni-Nb-O

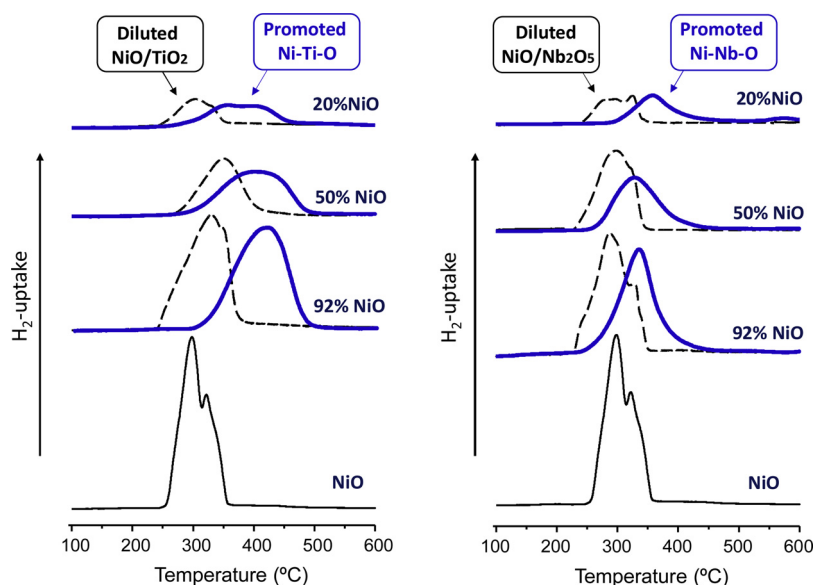


Fig. 7. TPR- H_2 profiles of promoted (blue) and diluted (black) NiO-based catalysts (For interpretation of the references to colour in this figure legend, the reader is referred to the web version of this article).

samples (i.e. the most selective catalysts in the ODH of ethane). For comparison, the XAS spectrum corresponding to metallic Ni is also included in this figure. A decrease in the “white line” intensity is observed for both 20NiO/TiO₂ and 92Ni-Nb-O samples, with respect to unselective NiO catalyst, likely due to a decrease in the average oxidation state of Ni atoms in modified catalysts [49]. More interestingly, it can be observed that the drop of the intensity is more drastic for promoted 92Ni-Nb-O than in the case of supported 20NiO/TiO₂. This goes in line with the previous observations, in which the modification of Ni species in NiO highly depends on the synthetic procedure chosen, although both diluters and promoters are able to improve the catalytic performance of NiO in the ODH of ethane.

According to these results, we can conclude that: i) promoters modify surface Ni sites in a higher extent than diluters, but; ii) both promoters and diluters are capable of eliminating the electrophilic oxygen species, which are responsible for total oxidation to carbon oxides. The main difference among diluted and promoted NiO-based catalysts is the amount of diluter/promoter necessary to achieve the proper interaction with the active phase, which leads to highly efficient materials in the ODH of ethane. Thus, especially due to the specific synthesis conditions, in which a more homogeneous distribution of Nb⁵⁺ and Ti⁴⁺ species can be assumed, the use of promoters requires much lower promoter contents (ca. 10 wt.%, i.e. a NiO concentration in the catalyst of ca. 90 wt.%), with respect to diluted catalysts, in which the amount of diluter must be much higher (ca. 80wt.%, i.e. a NiO content of ca. 20 wt. %) to achieve a comparable catalytic behavior in the ODH of ethane (i.e. selectivity to ethylene of about 90%).

The effect of both promoters and diluters on the reducibility of NiO-based catalysts was studied by means of temperature programmed reduction in H₂ (TPR- H_2). Fig. 7 compares TPR- H_2 profiles of selected promoted and diluted NiO catalysts. The samples show generally two clear reduction peaks, which can be associated to the two-step reduction of Ni²⁺ sites: Ni²⁺ → Ni^{δ+} → Ni⁰ [50]. It can be seen that both Nb- and Ti-promoted catalysts substantially shift the maximum consumption of hydrogen to higher temperatures, with respect to unmodified NiO (Fig. 7, blue profiles).

This indicates a decrease in the reducibility of nickel species present in promoted catalysts. This is considerably different in the case of TiO₂-P25 and Nb₂O₅-diluted materials, in which the reducibility does not vary significantly, according to the small variations in the TPR- H_2 profiles with respect to pure NiO (Fig. 7, black profiles).

Then, the reducibility of the catalysts seems to be related to the nature of nickel rather than to the type of oxygen species. According to XPS and XAS results, nickel species in diluted NiO catalysts seem to be more similar to those in pure NiO. This way, the reducibility of those sites will be equivalent in both cases. However, the elimination of electrophilic oxygen species takes place by both synthetic strategies, i.e. by promotion with high valence dopants (i.e. Nb⁵⁺ and Ti⁴⁺), or by the use of the corresponding diluter oxides (i.e. TiO₂-P25 or Nb₂O₅).

4. General remarks

During this work we have tried to shed some light into NiO-promoter and NiO-support interactions in NiO catalysts for the ODH of ethane. To cope with the problem, we have followed two synthetic approaches, by which nickel oxide has been promoted with Ti and Nb, or supported on TiO₂ and Nb₂O₅.

A similar NiO-promoter interaction has been observed in the case of Nb- and Ti-promoted catalysts. In this sense, XRD and Raman analyses suggest the isomorphous substitution of the promoter for Ni in nickel oxide framework, together with the formation of Ni-promoter mixed oxide phases, like ilmenite-type structure in the case of Ti-promoted NiO. A high interaction between nickel and both promoters can be also deduced from XPS and XAS studies, which suggest a decrease in the average oxidation state of nickel species and the elimination of electrophilic oxygen species (responsible for total oxidation of ethane). This leads to a decrease of the reducibility of the catalysts (as observed by TPR- H_2) and a drastic increase of the selectivity to ethylene (up to 90%) in the ODH of ethane at low promoter contents (92 wt. % of NiO).

On the other hand, TiO₂- and Nb₂O₅-diluted NiO materials show differences concerning the active phase-diluter interactions. Considering NiO/TiO₂ catalysts, they show the maximum selectivity to ethylene at low NiO-loading (i.e. high diluter contents). Then, a lower interaction with TiO₂ can be deduced with respect to Ti-promoted materials, although an outstanding performance in the ODH of ethane is achieved in both cases (ca. 90% selectivity to ethylene). This has been confirmed by XAS and XPS experiments. In this way, TiO₂ does not substantially modify the chemical nature of Ni sublattice, but it is able to eliminate the most electrophilic surface oxygen sites (non-selective sites). Consequently, the reducibility of diluted materials does not decrease so drastically with respect to pure NiO as it has been observed in Ti-promoted series.

Interestingly, Nb-diluted catalysts present low selectivity to ethylene in the ODH of ethane (48–68%). This behavior is observed regardless of the amount of NiO loaded. Their catalytic performance can be explained taking into consideration the low diluter-nickel interaction achieved. XPS measurements show that Nb₂O₅ is not able to eliminate non-selective electrophilic oxygen surface sites, associated to deep oxidation reaction path. In addition, the presence of Nb₂O₅ does not seem to modify the nature of surface Ni species.

5. Conclusions

Highly selective NiO-based catalysts for the ODH of ethane have been synthesized either by promoting NiO with Ti- or Nb- or by diluting NiO with TiO₂. However, Nb₂O₅-diluted NiO catalysts have not reached a satisfactory catalytic performance.

The catalytic behavior of promoted NiO catalysts seems to be dependent on the ability of the high valence dopants to be incorporated in the pristine NiO lattice. Thus, just low amounts of promoters are needed to eliminate non-selective active sites. On the other hand, in the case of diluted NiO catalysts, the modification of NiO mainly depends on the ability of the support to interact with nickel oxide particles. In this case, TiO₂ gives rise to a proper diluter-NiO interaction, although high TiO₂ contents are required to achieve an optimal catalytic performance. Conversely, Nb₂O₅ has not shown good properties as a NiO diluter, being unable to eliminate a large proportion of non-selective sites.

Acknowledgements

The authors would like to acknowledge the DGICYT in Spain (CRTI2018-099668-B-C21 and RTI2018-099668-B-C22 and MAT2017-84118-C2-1-R projects). Authors from ITQ also thank Project SEV-2016-0683 for supporting this research. D.D. thanks MINECO and Severo Ochoa Excellence Program for his fellowship (SVP-2014-068669).

Appendix A. Supplementary data

Supplementary data associated with this article can be found, in the online version, at <https://doi.org/10.1016/j.cattod.2019.06.063>.

References

- [1] A. Boulamanti, J.A. Moya, *Renew. Sustain. Energy Rev.* 68 (2017) 1205.
- [2] T. Ren, M. Patel, K. Blok, *Energy* 31 (2006) 425–451.
- [3] T. Ren, M.K. Patel, K. Blok, *Energy* 33 (2008) 817–833.
- [4] F. Cavani, N. Ballarini, A. Cericola, *Catal. Today* 127 (2007) 113–131.
- [5] J.M. López Nieto, B. Solsona, Gas phase heterogeneous partial oxidation reactions, in: J.C. Védrine (Ed.), *Metal Oxides in Heterogeneous Catalysis*, Elsevier, 2018, pp. 211–286.
- [6] J.M. Lopez Nieto, P. Botella, M.I. Vázquez, A. Dejoz, *Chem. Commun.* (2002) 1906–1907.
- [7] T.T. Nguyen, B. Deniau, M. Baca, J.-M.M. Millet, *Top. Catal.* 59 (2016) 1496–1505.
- [8] Y. Liu, US Patent US6355854 B1 (2001), assigned to Symyx Technologies Inc.
- [9] E. Heracleous, A.A. Lemonidou, *J. Catal.* 237 (2006) 162–174.
- [10] E. Heracleous, A.A. Lemonidou, *J. Catal.* 237 (2006) 175–189.
- [11] B. Solsona, J.M. López Nieto, P. Concepción, A. Dejoz, F. Ivars, M.I. Vázquez, *J. Catal.* 280 (2011) 28–39.
- [12] H. Zhu, D.C. Rosenfeld, M. Harb, D.H. Anjum, M.N. Hedhili, S. Ould-Chikh, J.-M. Basset, *ACS Catal.* 6 (2016) 2852–2866.
- [13] B. Solsona, P. Concepción, S. Hernández, B. Demicol, J.M. López Nieto, *Catal. Today* 180 (2012) 51–58.
- [14] H. Zhu, H. Dong, P. Lavelle, Y. Saih, V. Caps, J.-M. Basset, *Catal. Today* 228 (2014) 58–64.
- [15] H. Zhu, D.C. Rosenfeld, D.H. Anjum, S.S. Sangaru, Y. Saih, S. Ould-Chikh, *J. Catal.* 329 (2015) 291–306.
- [16] B. Solsona, P. Concepción, B. Demicol, S. Hernández, J.J. Delgado, J.J. Calvino, J.M. López Nieto, *J. Catal.* 295 (2012) 104–114.
- [17] D. Delgado, B. Solsona, A. Ykrelef, A. Rodríguez-Gómez, A. Caballero, E. Rodríguez-Aguado, E. Rodríguez-Castellón, J.M. López Nieto, *J. Phys. Chem. C* 121 (2017) 25132–25142.
- [18] Z. Skoufa, E. Heracleous, A.A. Lemonidou, *J. Catal.* 322 (2015) 118–129.
- [19] B. Savova, S. Loridant, D. Filkova, J.M.M. Millet, *Appl. Catal. A Gen.* 390 (2010) 148–157.
- [20] Z. Skoufa, E. Heracleous, A.A. Lemonidou, *Catal. Today* 192 (2012) 169–176.
- [21] H. Zhu, S. Ould-Chikh, D.H. Anjum, M. Sun, G. Biaisque, J.-M. Basset, V. Caps, *J. Catal.* 285 (2012) 292–303.
- [22] Z. Zhang, G. Zhao, R. Chai, J. Zhu, Y. Liu, Y. Lu, *Catal. Sci. Technol.* 8 (2018) 4383–4389.
- [23] E. Heracleous, A.F. Lee, K. Wilson, A.A. Lemonidou, *J. Catal.* 231 (2005) 159–171.
- [24] B. Solsona, P. Concepción, J.M. López Nieto, A. Dejoz, J.A. Cecilia, S. Agouram, M.D. Soriano, V. Torres, J. Jiménez-Jiménez, E. Rodríguez Castellón, *Catal. Sci. Technol.* 6 (2016) 3419–3429.
- [25] R. Sanchis, D. Delgado, S. Agouram, M.D. Soriano, M.I. Vázquez, E. Rodríguez-Castellón, B. Solsona, J.M. López Nieto, *Appl. Catal. A Gen.* 536 (2017) 18–26.
- [26] Z. Zhang, J. Ding, R. Chai, G. Zhao, Y. Liu, Y. Lu, *Appl. Catal. A Gen.* 550 (2018) 151–159.
- [27] E. Heracleous, A.A. Lemonidou, *J. Catal.* 270 (2010) 67–75.
- [28] J.M. López Nieto, B. Solsona, R.K. Grasselli, P. Concepción, *Top. Catal.* 57 (2014) 1248–1255.
- [29] D. Delgado, R. Sanchis, J.A. Cecilia, E. Rodríguez-Castellón, A. Caballero, B. Solsona, J.M. López Nieto, *Catal. Today* 333 (2019) 10–16.
- [30] C.A. Gärtner, A.C. van Veen, J.A. Lercher, *ChemCatChem* 5 (2013) 3196–3217.
- [31] S.W. Han, D.H. Kim, M.-G. Jeong, K.J. Park, Y.D. Kim, *Chem. Eng. J.* 283 (2016) 992–998.
- [32] M.-G. Jeong, I.H. Kim, S.W. Han, D.H. Kim, Y.D. Kim, *J. Mol. Catal. A Chem.* 414 (2016) 87–93.
- [33] B. Ohtani, O.O. Prieto-Mahaney, D. Li, R. Abe, J. Photochem. Photobiol. A 216 (2010) 179–182.
- [34] T. Murayama, J. Chen, J. Hirata, K. Matsumoto, W. Ueda, *Catal. Sci. Technol.* 4 (2014) 4250–4257.
- [35] A. Fernández-Arroyo, D. Delgado, M.E. Domine, J.M. López Nieto, *Catal. Sci. Technol.* 7 (2017) 5495–5499.
- [36] R.E. Dietz, G.I. Parisot, A.E. Meixner, *Phys. Rev. B* 4 (1971) 2302–2310.
- [37] J.M. Jehng, I.E. Wachs, *Chem. Mater.* 3 (1991) 100–107.
- [38] X. Wang, J. Shen, Q. Pan, *J. Raman Spectrosc.* 42 (2011) 1578–1582.
- [39] E. Rojas, J.J. Delgado, M.O. Guerrero-Pérez, M.A. Bañares, *Catal. Sci. Technol.* 3 (2013) 3173–3182.
- [40] L.J. Burcham, J. Datka, I.E. Wachs, *J. Phys. Chem. B* 103 (1999) 6015–6024.
- [41] M.A. Ruiz Preciado, A. Kassiba, A. Morales-Acevedo, M. Makowska-Janusik, *RSC Adv.* 5 (2015) 17396–17404.
- [42] P. Salagre, J.L.G. Fierro, F. Medina, J.E. Sueiras, *J. Mol. Catal. A Chem.* 106 (1996) 125–134.
- [43] J.C. Vedrine, G. Hollinger, D. Tran Minh, *J. Phys. Chem.* 82 (1978) 1515–1520.
- [44] V. Biju, M. Abdul Khadar, *J. Nanopart. Res.* 4 (2002) 247–253.
- [45] M.A. van Veenendaal, G.A. Sawatzky, *Phys. Rev. Lett.* 70 (1993) 2459–2462.
- [46] V.V. Kaichev, V.I. Bukhtiyarov, M. Hävecker, A. Knop-Gercke, R.W. Mayer, R. Schlögl, *Kinet. Catal.* 44 (2003) 432–440.
- [47] R.K. Grasselli, Fundamental principles of selective heterogeneous oxidation catalysis, *Top. Catal.* 21 (2002) 79–88.
- [48] J. Haber, Mechanism of heterogeneous catalytic oxidation, in: R.A. Sheldon, R.A. van Santen (Eds.), *Catalytic Oxidation: Principles and Applications*, World scientific, 1995, pp. 17–51.
- [49] J. Rabeah, J. Radnik, V. Briois, D. Maschmeyer, G. Stochniol, S. Peitz, H. Reeker, C. La Fontaine, A. Brückner, *ACS Catal.* 6 (2016) 8224–8228.
- [50] W. Shan, M. Luo, P. Ying, W. Shen, C. Li, *Appl. Catal. A Gen.* 246 (2003) 1–9.